Global Change Biology

Global Change Biology (2012) **18**, 642–655, doi: 10.1111/j.1365-2486.2011.02578.x

Trend changes in global greening and browning: contribution of short-term trends to longer-term change

ROGIER DE JONG*†, JAN VERBESSELT*, MICHAEL E. SCHAEPMAN‡ and SYTZE DE BRUIN*

*Laboratory of Geo-Information Science and Remote Sensing, Wageningen University, Droevendaalsesteeg 3, 6708PB, Wageningen, The Netherlands, †ISRIC – World Soil Information, Droevendaalsesteeg 3, 6708 PB, Wageningen, The Netherlands, ‡Remote Sensing Laboratories, University of Zurich, Winterthurerstrasse 190, CH-8057, Zurich, Switzerland

Abstract

Field observations and time series of vegetation greenness data from satellites provide evidence of changes in terrestrial vegetation activity over the past decades for several regions in the world. Changes in vegetation greenness over time may consist of an alternating sequence of greening and/or browning periods. This study examined this effect using detection of trend changes in normalized difference vegetation index (NDVI) satellite data between 1982 and 2008. Time series of 648 fortnightly images were analyzed using a trend breaks analysis (BFAST) procedure. Both abrupt and gradual changes were detected in large parts of the world, especially in (semi-arid) shrubland and grassland biomes where abrupt greening was often followed by gradual browning. Many abrupt changes were found around large-scale natural influences like the Mt Pinatubo eruption in 1991 and the strong 1997/98 El Niño event. The net global figure – considered over the full length of the time series – showed greening since the 1980s. This is in line with previous studies, but the change rates for individual short-term segments were found to be up to five times higher. Temporal analysis indicated that the area with browning trends increased over time while the area with greening trends decreased. The Southern Hemisphere showed the strongest evidence of browning. Here, periods of gradual browning were generally longer than periods of gradual greening. Net greening was detected in all biomes, most conspicuously in croplands and least conspicuously in needleleaf forests. For 15% of the global land area, trends were found to change between greening and browning within the analysis period. This demonstrates the importance of accounting for trend changes when analyzing long-term NDVI time series.

Keywords: GIMMS NDVI, global greening and browning, gradual and abrupt change detection, time series analysis, trend breaks

Received 24 May 2011; revised version received 9 September 2011 and accepted 15 September 2011

Introduction

Over the last few decades of the 20th century, terrestrial ecosystems acted as net carbon sink, as evidenced by ecosystem process models and satellite vegetation data (Myneni *et al*., 1997; Schimel *et al*., 2001; Zhou *et al*., 2001). The easing of climatic constraints on plant growth as a result of increased CO_2 concentrations and higher temperatures is a likely explanation for this effect (Nemani *et al*., 2003). Indications for increased biological activity were found in the Northern Hemisphere between 35° and 75° latitude (Zhou *et al*., 2001; Slayback *et al*., 2003) and in several hot spot regions, including the Sahel (Olsson *et al*., 2005; Fensholt *et al*., 2009) and parts of Australia (Donohue *et al*., 2009). On the other hand, many forested biomes experienced a decline in biological activity (De Jong *et al*., 2011a) and especially large parts of the boreal forests showed evidence of this, likely driven by late summer drought (Goetz *et al*., 2005). Since instrument measurements began, record high global mean temperatures were reached in the past decade (Hansen *et al*., 2010). This was found to induce a drying trend and a productivity decline in large parts of the Southern Hemisphere (SH), which counterbalanced the Northern Hemisphere (NH) green-up and resulted in a net global reduction in productivity (Zhao & Running, 2010). These findings may indicate a major change in the global greening regime. However, such trends may not be significant at large temporal extents and productivity estimates are often highly uncertain (Samanta *et al*., 2011). For this reason, there is a need to better understand the temporal and spatial dynamics of ecosystem productivity (Sjöström *et al*., 2011). The focus regarding such environmental changes is shifting toward increasingly large spatial and temporal extents (Niemi & Mcdonald, 2004; Pettorelli *et al*., 2005; Verbesselt *et al*., 2010a). As a result, long-term trends (i.e. time scales of decades) are becoming more likely to be composed of more extreme

Correspondence: Rogier de Jong, tel. + 31 0 317 483 734, fax + 31 0 317 419 000, e-mail: Rogier.deJong@wur.nl

shorter-term changes (i.e. several years), which might balance themselves out. An analysis of this effect at global scale is presented in this article.

A common way to derive indicators on environmental change is the use of spectral vegetation indices (Pettorelli *et al*., 2005). Such indices, based on the red/near infrared spectral region, are indicative of chlorophyll abundance and as such correlate to vegetation amount and photosynthetic capacity (Myneni *et al*., 1995). Positive and negative changes in time can be referred to as *greening* and *browning*, respectively. Here, time series of satellite data are particularly valuable because they provide a monitoring system with repeatable vegetation index (VI) measurements at scales at which climate- and human-induced changes take place (e.g. Wessels *et al*., 2007). Detecting changes within the time series is the first step toward assessing their environmental impact or attributing drivers or acting processes. Changes within VI time series can be divided into three major classes (Verbesselt *et al*., 2010a): seasonal changes, gradual changes, and abrupt changes. The first type occurs when the land surface phenology changes, e.g. driven by temperature or rainfall, without necessarily affecting the underlying trend component. For example, earlier onset of greening in spring might be counterbalanced by lower productivity late summer (Angert *et al*., 2005). The gradual and abrupt changes refer to the trend component beyond the seasonal variation. Slowly acting environmental processes, including climate change, certain land management practices or land degradation, may cause *gradual changes* in the time series. Over time, these gradual changes may stall or reverse (Scheffer *et al*., 2001; Zhao & Running, 2010), which involves a trend break. Following Verbesselt *et al.* (2010a), we define such an event, together with the associated magnitude and/or change in direction, as an *abrupt change*. Abrupt changes can also be induced by land use changes (Turner *et al*., 2007), wildfires (Kasischke *et al*., 1993; Boles & Verbyla, 2000), floods (Domenikiotis *et al*., 2003) or other fast-acting processes (Potter *et al*., 2003). This study focused on these abrupt and gradual VI changes.

Previous regional and global studies showed trends in vegetation activity using VI time series from spaceborne sensors like the American Advanced Very High Resolution Radiometer (AVHRR) and Moderate Resolution Imaging Spectrometer (MODIS) or the French VEGETATION sensor onboard Satellite Pour l'Observation de la Terre (SPOT). The direction and rate of change – together referred to as trend – have commonly been determined by the slope of a linear regression model in which the VI values or derived metrics depend on time (e.g. Paruelo *et al*., 2004; Herrmann *et al*., 2005; Olsson *et al*., 2005; Heumann *et al*., 2007; Bai *et al*., 2008). As a next step, trend changes may be considered within the analysis for closer relation to the system dynamics. In the case of trends in vegetation productivity since the early 1980s, many areas in the world are known or expected to show trend changes (Schimel *et al*., 2001; Slayback *et al*., 2003; Angert *et al*., 2005; Wang *et al*., 2011). For instance, trend changes were found in the early 1990s in the Northern Hemisphere (Slayback *et al*., 2003), possibly related to the June 1991 Mount Pinatubo eruption, which depressed incoming short-wave radiation and caused an anomalous cooling (Stenchikov *et al*., 1998; Lucht *et al*., 2002). Furthermore, the Northern Hemisphere greening seems to have stalled or even reversed toward browning in the last decade (Zhao & Running, 2010; Wang *et al*., 2011). There is a critical need for a consistent global assessment of trend changes within long-term vegetation time series. Here, we apply a data-driven change detection approach that is capable of quantifying trend changes without prior knowledge on location or timing. Regions in the world where trend changes have occurred are identified and net greening and browning for the 1982–2008 period is derived from a sequence of abrupt and gradual trend changes.

Methods

NDVI data

In an effort to monitor fluctuations in vegetation and understand interactions with the environment, the National Oceanic and atmospheric administration (NOAA) has been collecting images of vegetation condition using advanced very high resolution radiometer (AVHRR) sensors. The nonlinear combination of red and near infrared (NIR) spectral radiance (NIR − RED)/(NIR + RED), known as normalized difference vegetation index (NDVI), exhibits a strong relationship with green biomass and is commonly used for vegetation assessments from space (Tucker, 1979). For vegetated areas, infrared reflectance is higher than red reflectance and therefore NDVI ranges between 0 and 1 by definition.

The NOAA AVHRR sensors provide the longest available run of NDVI data, including the Global Inventory for Mapping and Modeling Studies (GIMMS) which was used in this study (Tucker *et al*., 2004). The data spans from 1981 through 2008 and has a temporal resolution of 2 weeks and a spatial resolution of 0.072 degrees (~8 km). Errors in NDVI introduced from orbital drift were largely (~90%) eliminated in the most recent GIMMS version (Tucker *et al*., 2005). The transitions between platforms may cause some discontinuities in the data (De Beurs & Henebry, 2005), but these are expected not to affect trend slopes (i.e. gradual changes) in the vegetation index (Kaufmann *et al*., 2000). A maximum value compositing (MVC) technique (Holben, 1986) was used to minimize cloud contamination during GIMMS processing and the risk of detecting trend changes caused by persistent cloud cover

was further reduced by the configuration of the trend break algorithm (see Methods section). Image acquisition started in July 1981, but we excluded 1981 to use only full 1-year periods in the analysis. In this way, the 27 year time series (1982–2008) for each pixel consists of 648 NDVI measurements with a frequency of 24 scenes per year.

The NDVI values lower than 0.2 are sparsely vegetated or not vegetated at all (Carlson & Ripley, 1997; Sobrino *et al.*, 2001), but to include sparsely vegetated areas in the analysis we masked pixels with yearly mean values below 0.1. The resulting dataset consists of 2,256,962 unmasked pixels (~86% of all terrestrial pixels excluding Antarctica). The NDVI signal in tropical evergreen forests is likely to saturate, causing low signal to noise ratios (Huete *et al.*, 1997). These regions were not omitted from the analysis, because abrupt changes might well be detectable. However, results for these regions were interpreted with caution.

Land cover classification

Detected vegetation changes were summarized per land cover class – which is also referred to as biome – because each might respond differently to climate change and to land use change (Chapin *et al.*, 2000; Verburg *et al.*, 2011). In the International Geosphere and Biosphere Programme (IGBP), a 1-km AVHRR-based land cover product (DISCover) intended for remote sensing of global change was developed (Loveland *et al.*, 2000). The dataset consists of 17 general land cover types, based on the climate-independent vegetation classification logic of Running *et al.* (1994), but extended to provide, where possible, land use implications and to represent landscape mosaics. For definitions of each category the reader is referred to Appendix 1 in Loveland & Belward (1997) and to Loveland *et al.* (2000) for an elaborated description of the dataset and comparison with other land cover datasets. The classification scheme, among few others, was later adopted within the (MODIS) land cover products. These products provide yearly land cover maps at 500 m spatial resolution. In this study, the MOD12C1 product (2009) was used, as it provides land cover at an aggregated 0.05 degree spatial resolution, which closely approaches the GIMMS spatial resolution. The original dataset was resampled using a majority method, which best preserves the spatial structure of major land cover classes at the cost of minor classes (Dendoncker *et al.*, 2008; Verburg *et al.*, 2011). For this reason, the class 'urban and built-up' had few pixels and was omitted from the summary statistics. The classes 'snow/ice', 'barren' and 'water bodies' are not represented in the analysis due to the masking procedure described in the NDVI data section.

Detecting trend changes within time series

Depending on biome, NDVI time series may contain a strong seasonal component linked with the growing seasons of vegetation being monitored. Most existing change detection techniques are unable to account for seasonal variation and analyze time series by aggregating the measurements by season or calendar year or they compare specific periods between years (Coppin *et al.*, 2004). A more generic change detection method was proposed by Verbesselt *et al.* (2010a,b). This method for detecting Breaks For Additive Seasonal and Trend (BFAST) accounts for seasonality and enables the detection of trend change within the time series. The methods are available in the BFAST package for R (R Development Core Team, 2011) from CRAN (http://cran.r-project.org/package=bfast). Here, we explain the key concepts of BFAST and apply a modified version. The full motivation for the procedure is given in afore-mentioned publications, where also a validation is provided using both simulated time series and MODIS NDVI data for Australian environments.

The basic principle of the BFAST algorithm is the combination of time series decomposition into seasonal, trend, and remainder components with methods for detecting structural changes in both the trend and seasonal components. In this study we focused on breaks in the trend component. It was assumed that nonlinearity can be approximated by a piecewise linear model and, as such, linearity was assumed in the individual trend segments. An additive decomposition approach was used to iteratively fit the piecewise linear regression model and a seasonal model (Haywood & Randall, 2008). The general model is of the form:

$$Y_t = T_t + S_t + e_t : t \in \{1 \ldots n\} \quad (1)$$

where, at time t in the time series $\{1 \ldots n\}$, Y_t is the observed NDVI value, T_t is the trend component, S_t the seasonal component en e_t the remainder component which contains the variation beyond what is explained by T_t and S_t.

The iteration is initialized with an estimate $\hat{S}_t$ of the seasonal component using a nonparametric season-trend decomposition (STL) method (Cleveland *et al.*, 1990). Subsequently, the estimates of S_t and T_t and their changes are determined by iterating through the following steps until the number and position of the detected breakpoints remain unchanged:

(step 1a) Test whether or not breakpoints occur in the seasonally adjusted data (Y_t–S_t), using the MOving SUM (MOSUM) approach (Zeileis & Kleiber, 2005). If the test indicates significant change ($\alpha = 0.05$), the breakpoints are estimated using the method of Bai & Perron (2003), as implemented by Zeileis *et al.* (2002). This method minimizes the Bayesian Information Criterion (BIC) (Schwarz, 1978) to determine the optimal number of breaks m and uses an iterative procedure – minimizing the residual sum of squares – to estimate the optimal break positions and accompanying 95% confidence intervals. For the MOSUM test to hold the nominal significance level, the error terms after decomposition should not be serially correlated.

(step 1b) The trend component $\hat{T}$ for each segment is estimated using robust linear regression (Venables & Ripley, 2002). As such, the trend component is described by a robust piecewise linear model, which allows the trend to exhibit changes. The positions in time of these trend changes are indicated by the

individual breakpoints, The trend within each segment j is assumed to be linear with intercept α_j and slope β_j:

$$T_t = \alpha_j + \beta_j \cdot t : j \in \{1 \ldots m+1\} \quad (2)$$

where m equals the number of abrupt trend changes so that m+1 equals the number of segments.

(step 2) Detrended data ($Y_t - T_t$) are used to refit the seasonal term S_t using a harmonic model with three components, i.e. periods of 12, 6, and 3 months.

(step 3) The number and position of breakpoints are compared to the previous iteration and the fitting procedure is finalized if they remain unchanged.

The BFAST can be generically applied to VI time series independent of the land cover type, reference periods or specific change trajectory. The only parameterization required is the maximum number of breakpoints m_{max} or the minimum time between breakpoints. The minimum time between breakpoints needs to coincide with the typical length scale of the monitored processes. In line with Verbesselt *et al.* (2010a) and following the recommendations of Bai & Perron (2003), we used a minimum of 4 years (corresponding to ~15% of the 27 year data span) between successive breakpoints. In case of several changes within a 4 year segment, only the most statistically significant is detected. This configuration also reduced the effect of persistently clouded areas, as clouds were found to be captured by the remainder component (e_t). For illustration, Figure 1 shows the decomposition and breakpoint detection for a GIMMS pixel in China. The trend component (T_t) consists of four segments with gradual changes, separated by three breakpoints at which abrupt changes were detected. For comparison, the T_t panel also shows the linear model for the entire time series, together with the slope coefficient and the corresponding significance value (P). The latter is based on generalized least squares (GLS) to account for remaining short-lag serial autocorrelation.

Analysis of NDVI changes

The BFAST procedure was extended to analyze the significance of the detected slopes in T_t against the null hypothesis that slope $\beta_j = 0$ at $\alpha = 0.05$ (degrees of freedom equals the number of observations in the segment minus 2). Only significant slopes were adopted as indicators for greening ($\beta_j > 0$) or browning ($\beta_j < 0$). Subsequently, the *duration* of the significant greening and browning segments and the *magnitude of change in NDVI* were calculated. The first is the sum of length of individual segments with significant slopes and the latter is a combination of gradual magnitude within segments and abrupt magnitude at the breakpoints between consecutive segments. Results were summarized at global, hemisphere, and biome scales. Abrupt changes shortly after the Mt Pinatubo eruption (Jun 1991–Dec 1992) were extracted to map possible effects of this eruption on NDVI trends. All described analyses

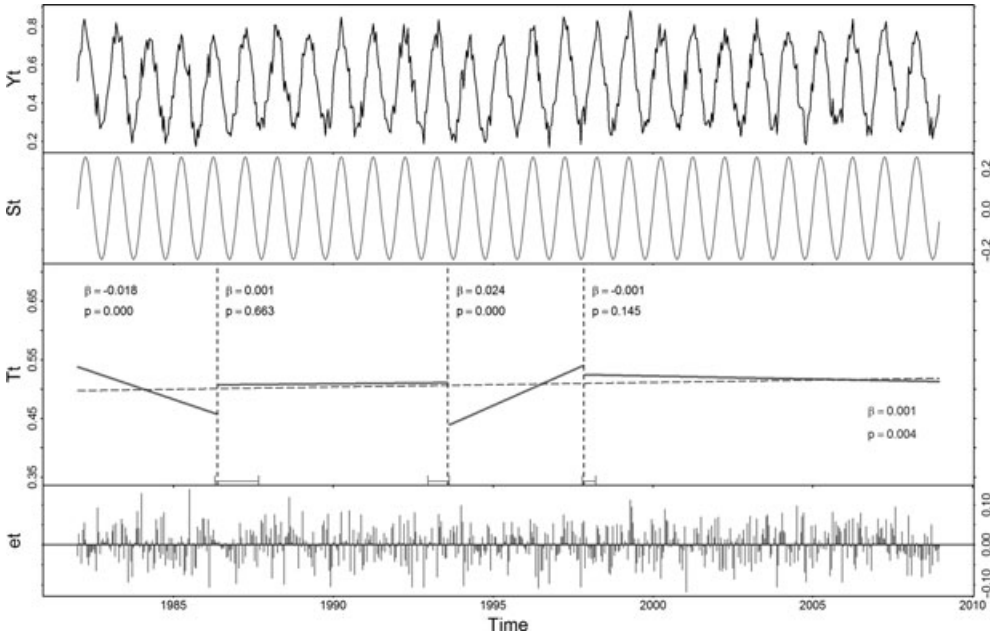

Fig. 1 Example of decomposition and trend break analysis for a location in China (35.913ºN, 108.513ºE). The top panel shows the global inventory for mapping and modeling studies normalized difference vegetation index (NDVI) data (Y_t), whereas the other three panels depict the individual components after decomposition. The seasonal (S_t) and remainder (e_t) components have zero mean while the trend component (T_t) shows the trend in NDVI: a period of browning between 1982 and 1986 and a period of greening between 1994 and 1998. The slope coefficients (β) of the other two segments are not significant ($P > 0.05$). The blue dashed line shows the equivalent linear model for the full time series.

were performed using R statistical software (R Development Core Team, 2011) on a high performance computing facility.

Results

Duration of gradual changes

Figure 2 illustrates the detected duration of both gradual greening and gradual browning, without showing the associated slope or absolute changes in NDVI values. The most conspicuous region in terms of long greening periods is the eastern part of Europe. Also regions in North America, most tundra regions, the savanna between the Sahara desert and the equator, and parts of India exhibited a greening trend for 20 years or longer. Most of these areas are in the Northern Hemisphere while long browning periods were mainly found in the Southern Hemisphere, conspicuously in parts of Argentina and Australia. In the

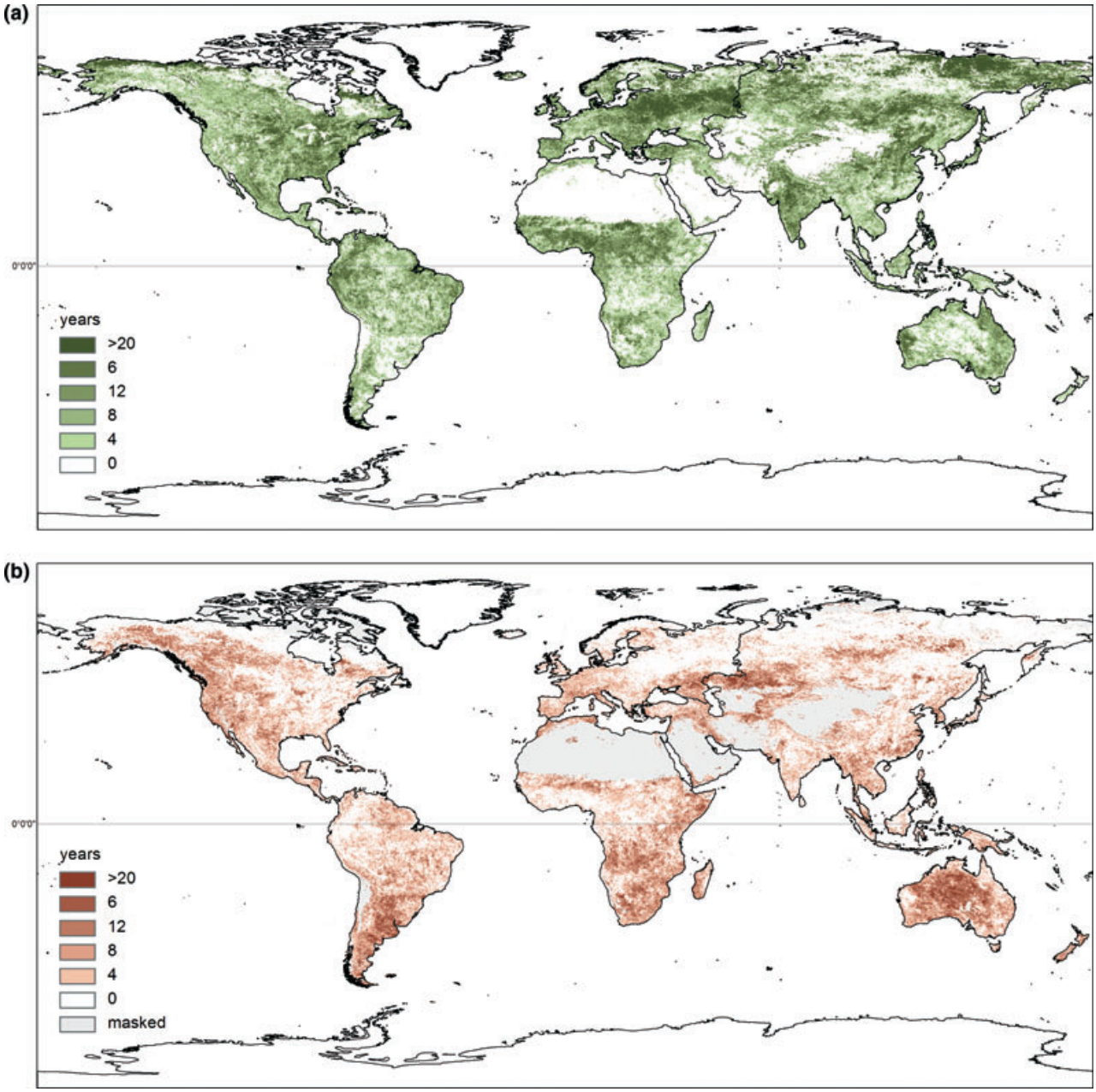

Fig. 2 Duration of change by means of number of years in which a significant normalized difference vegetation index trend was found ($\alpha = 0.05$). (a) positive trend, or greening and (b) negative trend, or browning. White areas were masked out (see sections Data and Methods) or showed insignificant trends.

Northern Hemisphere, on the other hand, browning was mainly found in the Kazakh steppe and in the boreal forests in parts of Siberia, Alaska, and Canada.

A distinct difference was found between both hemispheres regarding the duration of greening and browning. Gradual greening trends lasted longer than equivalent browning trends in all biomes in the Northern Hemisphere, whereas the opposite holds for most biomes in the Southern Hemisphere (Table 1). The global figure is mainly determined by the Northern Hemisphere – due to the north-heavy arrangements of the continents – and therefore greening trends lasted longer in all biomes, although most conspicuously in mixed forests, croplands, and cropland/vegetation mosaics. The longest gradual browning trends were found in grasslands. On average, the detected duration of gradual changes varied roughly between 3 and 6 years for NH browning and between 9 and 14 years for NH greening. The SH durations varied between 7 and 9 years for greening and between 7 and 12 years for browning.

Trend breaks

Following the described approach, large parts of the global surface experienced NDVI trend changes during the 1982–2008 period. From the unmasked area, 32.9% shows zero, 27.2% one, 22.7% two, and 17.2% more trend changes. Most of these were detected in Australia, Argentina, south-west Texas (USA)/north-east Mexico, Botswana, and western South Africa (Fig. 3). The higher northern latitudes and the tropics seem least affected by trend discontinuities, although some were detected in the North American boreal forests. For the better part, the detected breakpoints separate segments with significant slopes from segments with insignificant slopes. However, for 14.5% of the total land surface the slope coefficient swapped sign, which indicates that both a period of significant greening and a period of significant browning occurred at the same location between 1982 and 2008. Many of these shifts between greening and browning were found not only in semi-arid climate regions, but also in temperate climate regions in Europe and North America. The majority of this area corresponded to open and closed shrubland, whereas grassland takes a second place.

Magnitude of NDVI changes

Global greening and browning patterns were divided into gradual and abrupt changes in NDVI and are shown in Figure 4a, b. Gradual changes – which are calculated from the detected duration of change and the corresponding slope coefficients – are shown in green and brown colors, respectively, and abrupt changes at breakpoints are, partially transparent, shown in blue. The magnitude of each of these components varies between 0 and ~0.15 (absolute NDVI units). Greening was found in many parts of the world and most conspicuously in the Northern Hemisphere, which is in line with the longer change trajectories of greening found there (Table 1). Abrupt greening was mainly found in areas with relatively sparse vegetation cover (e.g. Australian rangelands, African open shrub-

Table 1 Total duration of gradual normalized difference vegetation index change in years. Lengths of individual significant segments were summed and averaged over all pixels within the land cover class for the Northern Hemisphere, the Southern Hemisphere and globally. Land cover classes (number and name) are according to the International Geosphere and Biosphere Programme classification (Loveland *et al.*, 2000)

		Positive change (greening)			Negative change (browning)		
Land cover class/biome		*NH*	*SH*	*G*	*NH*	*SH*	*G*
1	Evergreen needleleaf forest	10.41		10.41	6.14		6.14
2	Evergreen broadleaf forest	9.51	9.48	9.51	5.24	7.34	5.05
3	Deciduous needleleaf forest	7.84		7.84	4.21		4.21
4	Deciduous broadleaf forest	13.08	6.56	11.10	4.25	9.76	6.00
5	Mixed forests	13.57		13.57	4.04		4.04
6	Closed shrublands	10.32	9.70	10.13	6.21	9.67	7.55
7	Open shrublands	11.93	7.58	10.75	2.93	12.44	5.43
8	Woody savannas	9.83	7.14	9.16	4.76	8.87	5.81
9	Savannas	14.98	9.18	10.34	3.92	7.54	6.83
10	Grasslands	10.77	7.59	10.18	7.85	10.55	8.34
11	Permanent wetlands	12.10	7.70	11.38	3.02	8.27	3.74
12	Croplands	13.49	8.10	12.86	5.09	10.23	5.66
14	Cropland/vegetation mosaic	13.31	8.68	12.60	4.46	6.70	4.78

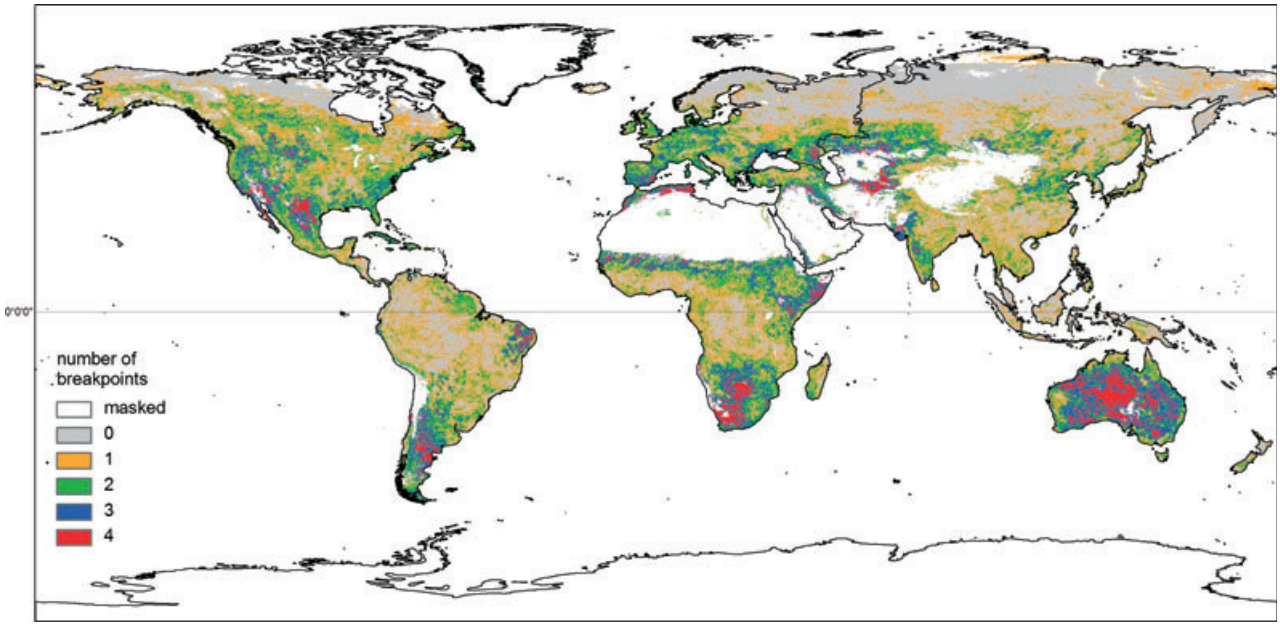

Fig. 3 Number of detected abrupt changes, or breakpoints, irrespective of the magnitude of the changes. Areas with a yearly mean normalized difference vegetation index < 0.10 were masked out.

lands, and the Sahel region), mostly in combination with gradual browning, whereas abrupt browning was mainly detected in more densely vegetated regions (e.g. broadleaf forest in Europe and North America) and in humid grasslands. The sum of all significant change components provides the net change in NDVI (Fig. 4c), with magnitudes up to ~0.04 (absolute NDVI units).

Table 2 summarizes the detected changes in NDVI per biome and hemisphere. At global scale, Net greening is most conspicuous in cropland regions (net change 0.034), followed by evergreen broadleaf and mixed forests. In the Northern Hemisphere, savannas show the strongest indication for greening (0.050). Net greening was found in all biomes except for few minor net browning changes in the Southern Hemisphere. In general, the Northern Hemisphere shows less variation (in terms of absolute greening and browning per biome), but higher net NDVI changes compared to the Southern Hemisphere. In the latter, the highest variation was detected in shrublands and grasslands (e.g. parts of the Australian rangelands, Andean puna, and Patagonian steppe/Monte semi-desert). The lowest variation was found in needleleaf forest and open shrublands in the Northern Hemisphere (e.g. boreal forest and tundra).

The detected NDVI trends do not only vary in space, but also in time. Figure 5 illustrates how gradual greening and browning trends were found to evolve across the time series by means of globally aggregated area per fortnightly time-step (with respect to the first 4 years in which no trend changes occurred by definition). It appeared that the area which showed gradual greening decreased to 83% (with respect to the start of the time series) between 1986 and 2002, after which it increased to 92%. The browning area quickly increased to 118% in 1994, after which is decreased and stabilized around 110%. The total land area which experienced gradual changes was found to vary between 51% and 56% (blue line) with the minimum around the year 2000.

Discussion

The presented methodology, based on the BFAST algorithm, enabled detection of short-term greening or browning periods within a longer time series of satellite data. This approach is, in this sense, more flexible than previous global assessments of vegetation activity (Bai *et al.*, 2008; De Jong *et al.*, 2011a). There is general agreement with respect to the afore-mentioned global assessments regarding the spatial pattern of net changes in NDVI (Fig. 4c). However, the results showed different spatial patterns for gradual and abrupt NDVI changes (Fig. 4a, b) and indicated that gradual trends generally last for periods shorter than the full length of the time series (Fig. 2). The change rates for these shorter periods were, by definition, greater than those found using monotonic analysis and resulted in higher absolute NDVI changes within the 1982–2008 time span (Table 2). Considered over all

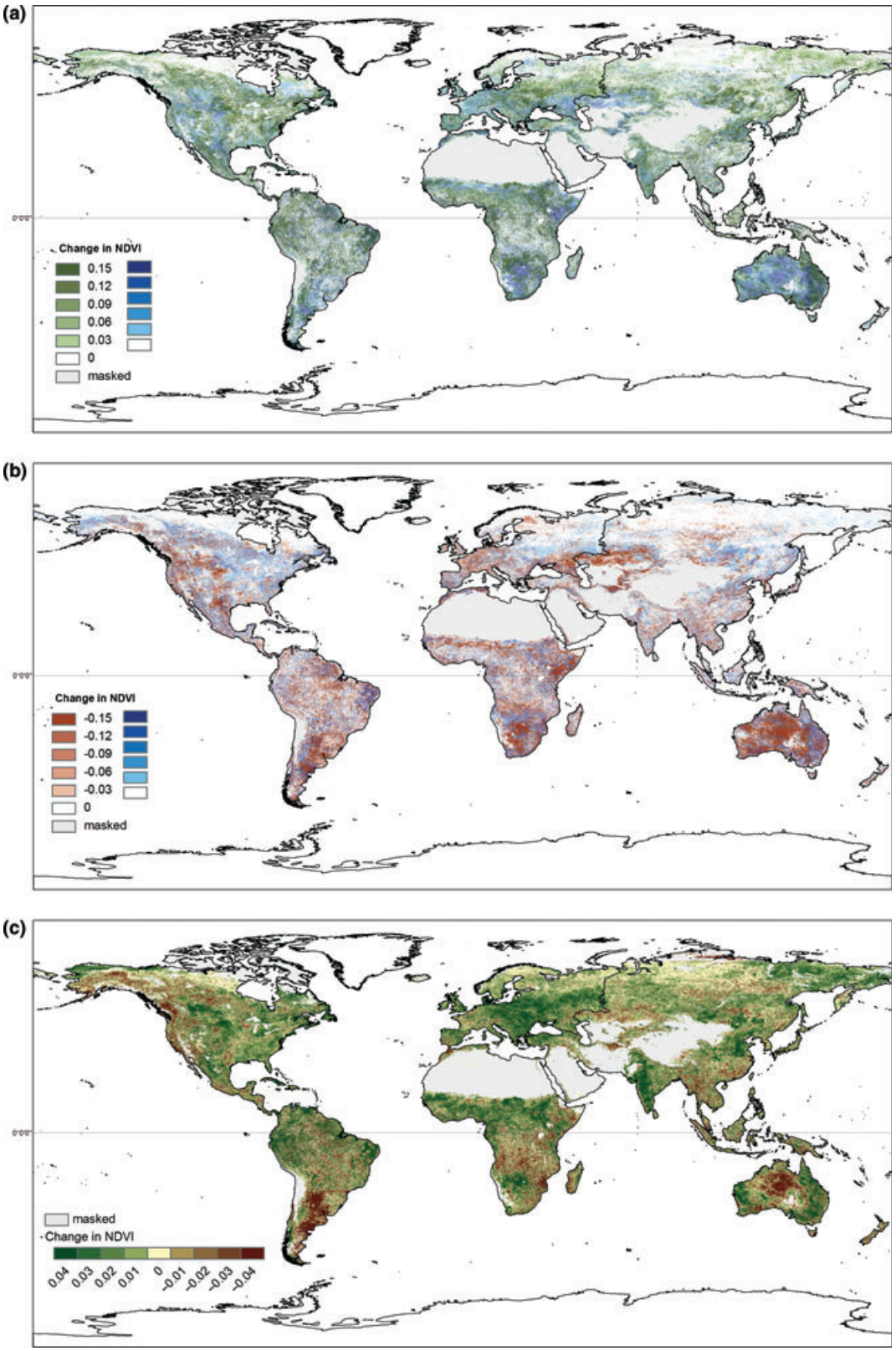

Fig. 4 Global greening and browning in terms of normalized difference vegetation index changes between 1982 and 2008: (a) positive changes, both gradual (green) and abrupt (blue); (b) negative changes, both gradual (red) and abrupt (blue); (c) sum of the four components of figures a and b.

Table 2 Absolute changes in normalized difference vegetation index for the time span of the Global Inventory for Mapping and Modeling Studies dataset (1982–2008), subdivided into abrupt and gradual changes for the Northern Hemisphere, the Southern Hemisphere, and globally. For easier numerical representation, values were multiplied by 100. Land cover classes (number and name) are according to the International Geosphere and Biosphere Programme classification (Loveland *et al.*, 2000)

		Gradual change			Abrupt change			Net result		
Land cover class/biome		*NH*	*SH*	*G*	*NH*	*SH*	*G*	*NH*	*SH*	*G*
Greening										
1	Evergreen needleleaf forest	5.80		5.92	2.91		2.91	0.68		**0.81**
2	Evergreen broadleaf forest	9.23	9.24	9.25	5.87	5.99	5.94	2.25	2.65	**2.50**
3	Deciduous needleleaf forest	3.10		3.10	1.18		1.18	0.81		**0.82**
4	Deciduous broadleaf forest	7.38	7.62	7.56	3.59	6.29	4.46	2.56		**1.53**
5	Mixed forests	5.89		6.05	2.58		2.58	2.45		**2.61**
6	Closed shrublands	7.74	12.10	9.60	6.61	11.97	8.75	2.02	0.28	**1.42**
7	Open shrublands	3.71	7.47	4.67	2.39	13.17	5.22	1.90	0.02	**1.39**
8	Woody savannas	5.09	9.08	6.13	2.79	6.25	3.67	1.39	0.44	**1.16**
9	Savannas	9.84	10.84	10.65	5.68	6.81	6.59	5.03	1.67	**2.33**
10	Grasslands	6.00	8.03	6.32	6.40	9.58	6.96	2.04		**1.55**
11	Permanent wetlands	4.39	7.94	4.77	2.68	5.68	3.05	2.34	0.43	**2.07**
12	Croplands	7.84	10.84	8.14	4.62	8.06	5.01	3.79	0.36	**3.40**
14	Cropland/vegetation Mosaic	7.09	7.23	7.10	3.73	4.66	3.85	2.87	1.08	**2.62**
Browning										
1	Evergreen needleleaf forest	−3.75		−3.74	−4.28		−4.28			
2	Evergreen broadleaf forest	−6.42	−6.55	−6.48	−6.43	−6.03	−6.21			
3	Deciduous needleleaf forest	−1.42		−1.42	−2.04		−2.04			
4	Deciduous broadleaf forest	−3.34	−8.36	−4.98	−5.08	−6.33	−5.51		−0.79	
5	Mixed forests	−2.53		−2.53	−3.49		−3.49			
6	Closed shrublands	−6.84	−14.69	−9.94	−5.50	−9.09	−6.99			
7	Open shrublands	−2.32	−14.79	−5.60	−1.88	−5.83	−2.90			
8	Woody savannas	−3.03	−7.56	−4.19	−3.47	−7.33	−4.46			
9	Savannas	−4.99	−7.48	−6.99	−5.50	−8.50	−7.91			
10	Grasslands	−6.49	−11.67	−7.41	−3.87	−6.52	−4.32		−0.58	
11	Permanent wetlands	−2.22	−7.20	−2.83	−2.52	−5.99	−2.92			
12	Croplands	−4.12	−10.41	−4.81	−4.55	−8.14	−4.93			
14	Cropland/vegetation mosaic	−3.59	−5.55	−3.85	−4.36	−5.25	−4.48			

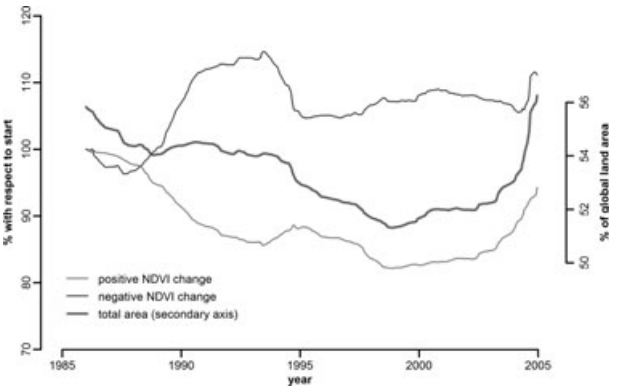

Fig. 5 Primary axis: area with positive gradual trends in normalized difference vegetation index (*greening*) and negative gradual trends (*browning*) over time. The area was indexed with respect to the first 4 years (minimal segment length) of the time series. Secondary axis: percentage of total land area with significant greening or browning trend.

pixels used in this study, greening rates were found to be around 4–5 times greater with respect to monotonic analysis with a fixed change duration of 26 years (Bai *et al.*, 2008). Browning rates were also greater, which is mainly accountable to shrubland biomes. This indicates that, especially in these regions, short-term greening and browning effects are averaged out using monotonic analysis. The latter was found to occur in approximately 15% of the global land area, which showed both gradual browning and gradual greening trends between 1982 and 2008. The net global figure of NDVI change was positive for all land cover classes, but slightly lower than estimated in mentioned monotonic studies. A plausible explanation for this effect is that monotonic methods are likely to overestimate changes in periods which were considered stable in this study. For example, in Figure 1 the entire time span was considered significant in case of the monotonic method

(P = 0.004), while only ~9 out of 27 years were considered significant using the BFAST method.

Possible drivers of NDVI trends and trend changes

Terrestrial vegetation productivity is influenced by many cyclical and abrupt events which might cause trends in vegetation productivity to change (Gobron *et al.*, 2010). These events include not only climatic and oceanic oscillations, of which the El Niño/La Niña – Southern Oscillation (ENSO) with a period of 4–7 years is the best known (Woodward *et al.*, 2008), but also volcanic eruptions and anomalously warm and dry years (e.g. the European drought of 2003: Ciais *et al.*, 2005). Aside from biophysical drivers, the observation record might be contaminated with measurement errors originating from sensor changes, orbital drift of satellites or atmospheric effects. Most measurement errors can be well corrected for, but other drivers are likely to cause actual changes in vegetation response in some biomes or regions (e.g. volcanic eruptions and oceanic oscillations). Some of these effects are discussed herein.

The GIMMS dataset has been corrected for aerosols injected into atmosphere by volcanic eruptions, i.e. the El Chichon eruption in April 1982 and the Mount Pinatubo eruption in June 1991 (Slayback *et al.*, 2003). Still, discontinuities might result from actual vegetation response to temporary global cooling. Effects of El Chicon are not likely to be found in the GIMMS data, because the eruption date is close to the start of the dataset and therefore the initial status is unknown. After the Mt Pinatubo eruption, however, a higher representation of breakpoints was found (De Jong *et al.*, 2011b) and cooling effects attributable to the eruption have been reported around the world (Lucht *et al.*, 2002; Soden *et al.*, 2002; Angert *et al.*, 2004). This provides a candidate explanation for the high occurrence of abrupt trend changes around this time. Figure 6 shows that abrupt changes in NDVI were detected in many regions in the world between June 1991 and December 1992. Browning was most conspicuous in North America, Southern Africa, and Eastern Asia. This corresponds with negative NDVI changes found in the higher northern latitudes between 1991 and 1992 (Slayback *et al.*, 2003). Two large regions showed positive changes (abrupt greening): Kazakhstan and the states of Western and South Australia. In Kazakhstan this might be explained by a sharp decline in precipitation in the years before the eruption (Pilifosova *et al.*, 1997). A weak El Niño event caused warming and higher precipitation in certain regions shortly after the eruption date (Woodward *et al.*, 2008). This might have counterbalanced some Pinatubo effects and caused the abrupt greening in Australia.

The Sahel experienced climatic extremes in terms of drought. During the last 30 years of the 20th century, nearly all years have been anomalously dry (Nicholson, 2000), which is likely related to the Atlantic multidecadal oscillations (AMO) (Zhang & Delworth, 2006). In water-limited ecosystems like these, such rainfall trends are expected to induce browning trends, possibly amplified by a positive feedback due to increasing

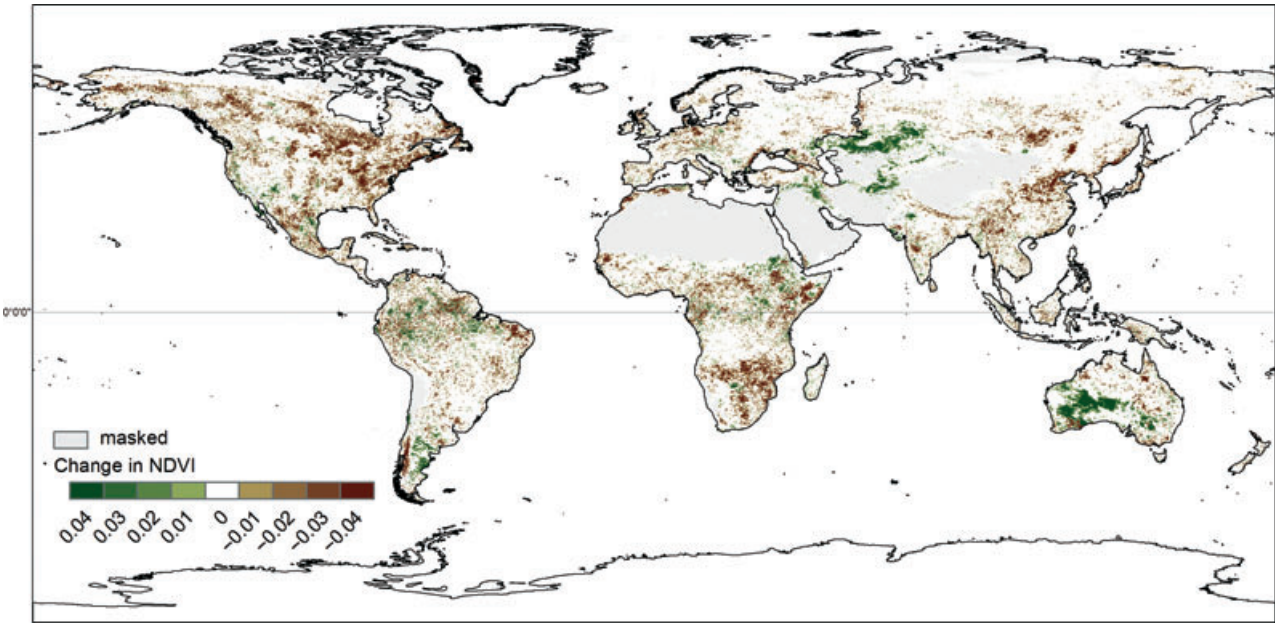

Fig. 6 Magnitude of abrupt normalized difference vegetation index changes detected shortly after the Mt Pinatubo eruption (June 1991–December 1992). Green colors indicate positive changes and brown colors negative changes.

albedo (Zhang & Delworth, 2006). However, greening trends were found in the Sahel, especially in the southern parts. These trends are strongest in the 1980s and were found to change into browning trends in the northern Sahel. The net result for 1982–2008 showed greening (Fig. 4c), which is probably the result of recovery from the droughts which were most severe around the start of the GIMMS dataset. It will be a complex exercise to disentangle all sea-atmosphere-land interactions which drive the gradual and abrupt changes in vegetation productivity, but there seems to be a general agreement that the Sahel vegetation is heavily influenced by natural processes, more than by men (Fensholt & Rasmussen, 2011). In these and other shrubland biomes – especially in the Southern Hemisphere – it was found that the greening changes are generally abrupt, followed by gradual browning (Fig. 4 and Table 2, classes 6 and 7). Relatively wet years might lead to extensive germination of short-lived plants, which is followed by browning in successive drier years. The total variation in NDVI is also highest in these regions (together with grasslands) which is likely explained by strong reactions to climatic fluctuations like ENSO cycles. A large number of abrupt changes were found in Australia – which is particularly prone to ENSO fluctuations – around the strong 1997/98 El Niño (Wolter & Timlin, 1998) and following La Niña events. These fluctuations are much smaller in the Northern Hemisphere figures for the same biomes, owing to the stable tundra regions, which form – in the IGBP DISCover classification – part of the (open) shrublands and due to the reduced ENSO influences. Other climatic oscillations which act at (sub-) decadal time scale and which have larger effects in the Northern Hemisphere include the Pacific Decadal Oscillation (PDO) and the North Atlantic Oscillation (NAO). Both have mainly been in positive phases during the GIMMS time span, which lead to relatively high temperatures in some regions (Viles & Goudie, 2003), but not likely to trend breaks in NDVI.

Relatively long periods of browning were detected in boreal forests in Canada and Siberia (Fig. 2). This boreal browning is in line with results from previous studies (Bunn *et al*., 2007), in which drought and, accordingly, vapor pressure deficits (VPD) were documented as possible drivers. In North America, large forested areas experienced a decline in productivity without significant changes in growing season length, indicating impacts of late summer drought (Zhang *et al*., 2009; Goetz *et al*., 2011). This is in agreement with several trend analyses performed on the GIMMS dataset indicating that boreal browning is mainly attributable to stress within the growing season, rather than to changes in length of growing season (Goetz *et al*., 2005; De Jong *et al*., 2011a) and supported by tree ring studies (Lloyd & Bunn, 2007). Net NDVI increase was found for all land cover classes, but Table 2 shows that the lowest increases were found for needleleaf forest – which is most abundant in the boreal regions. Arctic coastal tundra ecosystems, on the other hand, mostly show a stable greening trend which is likely related to decreasing sea ice concentrations and associated higher land surface temperatures (Goetz *et al*., 2011). Aside from boreal regions, long periods of browning were also found in Kazakhstan. These have been attributed to drought conditions, at least toward the end of the time series as negative precipitation trends were found from both station observations and gridded precipitation data (De Beurs *et al*., 2009). The same research showed an increase in NDVI, using MODIS data from 2000–2008, in a study area in the European part of Russia, which is in accordance with the long-term greening trends found in this study. These trends were attributed to land abandonment and an increase in agricultural productivity (De Beurs *et al*., 2009). Agricultural expansion plays an important role in Argentina as well (Viglizzo *et al*., 2011), which is likely one of the drivers of the negative NDVI trends found there. On the other hand, the strongest indication for greening is also found in cropland regions (Table 2), which is likely attributable to improved agricultural techniques. Urban expansion might have caused local NDVI decline around several cities. In the global statistics this effect is not captured as a result of the resampling scheme used for the land cover data. For such purposes it is recommended to run the BFAST algorithm on MODIS (or equivalent) data. This recommendation also holds for other purposes where processes act beyond the spatial resolution of GIMMS, for instance most deforestation studies.

Many regions, other than those discussed above, show significant NDVI trends and for most of these regions ample studies relate the trends to possible drivers. Few studies, however, assessed trends and drivers at continental or larger scale. In the Northern Hemisphere, greening patterns were found and related to increasing temperature and precipitation (Zhou *et al*., 2001), but recently trends in certain regions were also found to have stalled or even inversed (Wang *et al*., 2011). Globally, the terrestrial net primary productivity (NPP) was found to have reduced during the past decade, attributable to large-scale warming-associated droughts in the Southern Hemisphere (Zhao & Running, 2010) and a likely soil moisture deficit (Jung *et al*., 2010). This is in line with the browning patterns (Table 2) and the increasing area with browning trends (Fig. 5) found in this study, although the strongest increase was found before 1994. The sharp increase in

2004 might be partly explained by a decrease in vegetation productivity in Europe following the anomalous warm year of 2003 (Ciais *et al*., 2005). Overall, the past decade showed an increase in greening trends, but our analysis period for trend changes was limited to 2005.

Limits and artifacts

The presented approach proved capable of detecting trend changes in global NDVI time series, which reduced the limitation of a commonly assumed fixed change trajectory. Common trend analysis methods may average out the temporal signal for time series which consist of several different change periods. Accordingly, areas might be labeled stable while in reality changes might have occurred over periods of several years or – the other way around – stable periods are included in a significant long-term trend. The longer a time series is, the more likely that this effect conceals actual short-term trends, which might be more valuable for establishing relationships with driving processes than those for long-term trends. Information on greening vs. browning sign changes, for instance, is crucial for monitoring the effect of land management changes or the influence of meteorological conditions on vegetation status. This information can be provided using the presented approach, keeping in mind some constraints.

Several NOAA satellites have been used to generate the GIMMS dataset. Although the data have been thoroughly corrected (Tucker *et al*., 2005), this potentially causes trend breaks within the time series (Cracknell, 1997; De Beurs & Henebry, 2004). Table 3 lists the platform changes and the corresponding dates. We analyzed the frequency distribution of the detected break points, from which it appeared that few sensor changes (between NOAA platforms 9, 11 and 14) coincide with periods with a higher than average number of breakpoints (De Jong *et al*., 2011b) but a causal relationship could not be established. The likeliness of these transitions influencing the timing of detected breaks is highest in low-latitude biomes, especially in case of sparse vegetation cover and relatively light-colored soils, but even then it is likely not to affect the detected trend slopes (Kaufmann *et al*., 2000).

Table 3 Sensor changes within the time span of the Global Inventory for Mapping and Modeling Studies dataset. Due to malfunction of National Oceanic and atmospheric administration (NOAA)-11 and failure of NOAA-13 to achieve orbit, NOAA-9 descending node data was used in the period September 20, 1994 until January 19, 1995 (Tucker *et al*., 2005)

AVHRR platforms	Date
NOAA-7 > NOAA-9	Feb 10, 1985
NOAA-9 > NOAA-11	Nov 9, 1988
NOAA-11 > NOAA-9d	Sep 20, 1994
NOAA-9d > NOAA-14	Jan 19, 1995
NOAA-14 > NOAA-16	Nov 1, 2000
NOAA-16 > NOAA-17	Jan 1, 2004

NDVI is a one dimensional measure with a multidimensional biophysical origin, which – despite the improved time series analysis techniques – urges caution in the interpretation of trends. Given that the data are free of measurement errors, it still does not directly measure the amount of standing biomass nor the vegetation productivity, but is also influenced by canopy structure and soil parameters, among others (Baret & Guyot, 1991; Myneni *et al*., 1995). It is therefore not straightforward to relate NDVI changes to ecosystem changes, which in itself are often multi-actor issues and subject to change over time (Nelson *et al*., 2006). Expressing productivity change in terms of Net Primary Productivity (NPP) – using empirical relationships with NDVI or production efficiency models – yields an indicator which is closer related to biophysical processes and better amenable to economic analysis. The relationship between the two, however, is not always strong and not over the entire range linear (Paruelo *et al*., 1997), although a large part of interannual variation in NPP (30% up to 90%, depending on biome) can be explained by NDVI (Potter *et al*., 1999). The application of trend break analysis of satellite records in combination with production efficiency models needs further investigation.

Conclusions

Temporal decomposition of trends in vegetation activity inferred from NDVI revealed an alternating pattern of short-term greening and browning trends for large parts of the terrestrial surface. For almost 15% of this area, both periods with an increase and with a decrease in vegetation activity were found between 1982 and 2008. The ENSO-prone shrubland and grassland regions, mainly in the Southern Hemisphere, appeared specifically prone to reversing trends. Many trend changes were detected for certain regions after the strong ENSO event of 1997/98 and globally after the Mt Pinatubo eruption of June 1991.

Different spatial patterns were found for abrupt and gradual changes. Abrupt greening prevailed in semiarid regions, probably due to their strong reactions to climatic variations. These abrupt greening events were often followed by periods of gradual browning. In general, greening prevails in all land cover classes and as a result the global figure indicates greening between 1982 and 2008. The strongest indication for this was found in croplands and the weakest in needleleaf forests.

Greening trends were also found to be weaker in the Southern Hemisphere, compared to the Northern Hemisphere. Globally, the area which experienced gradual greening trends was found to decrease over time, while browning increased. This might indicate an overall reduction in global terrestrial vegetation activity, although an increasing trend was found in recent years.

The results from this study show that linear trend analysis over a time series of arbitrary length may obscure significant trend changes appearing within shorter duration, while particularly the latter can be linked to large-scale drivers. As such, automatic detection of trend changes provides a new step in the analysis of trends in global vegetation activity, specifically in (semi-arid) shrub- and grassland biomes.

Acknowledgements

We are grateful to Molly Brown and the GIMMS group for providing their latest dataset and to the ESG-HPC people of Wageningen University for facilitating model calculations. We acknowledge in particular Wietse Franssen for his assistance. We thank Achim Zeileis for his answers to our questions about structural change and three anonymous reviewers and the editor for their constructive comments, which helped to improve the manuscript.

References

Angert A, Biraud S, Bonfils C, Buermann W, Fung I (2004) CO_2 seasonality indicates origins of post-Pinatubo sink. *Geophysical Research Letters*, **31**, L11103.

Angert A, Biraud S, Bonfils C *et al.* (2005) Drier summers cancel out the CO_2 uptake enhancement induced by warmer springs. *Proceedings of the National Academy of Sciences of the United States of America*, **102**, 10823–10827.

Bai J, Perron P (2003) Computation and analysis of multiple structural change models. *Journal of Applied Econometrics*, **18**, 1–22.

Bai ZG, Dent DL, Olsson L, Schaepman ME (2008) Proxy global assessment of land degradation. *Soil Use and Management*, **24**, 223–234.

Baret F, Guyot G (1991) Potentials and limits of vegetation indices for LAI and APAR assessment. *Remote Sensing of Environment*, **35**, 161–173.

Boles SH, Verbyla DL (2000) Comparison of three AVHRR-based fire detection algorithms for interior alaska. *Remote Sensing of Environment*, **72**, 1–16.

Bunn AG, Goetz SJ, Kimball JS, Zhang K (2007) Northern high-latitude ecosystems respond to climate change. *Eos*, **88**, 333–340.

Carlson TN, Ripley DA (1997) On the relation between NDVI, fractional vegetation cover, and leaf area index. *Remote Sensing of Environment*, **62**, 241–252.

Chapin FS, Zavaleta ES, Eviner VT *et al.* (2000) Consequences of changing biodiversity. *Nature*, **405**, 234–242.

Ciais P, Reichstein M, Viovy N *et al.* (2005) Europe-wide reduction in primary productivity caused by the heat and drought in 2003. *Nature*, **437**, 529–533.

Cleveland RB, Cleveland WS, Mcrae JE, Terpenning I (1990) STL: A seasonal-trend decomposition procedure based on loess. *Journal of Official Statistics*, **6**, 3–73.

Coppin P, Jonckheere I, Nackaerts K, Muys B, Lambin E (2004) Digital change detection methods in ecosystem monitoring: a review. *International Journal of Remote Sensing*, **25**, 1565–1596.

Cracknell AP (1997) *The Advanced Very High Resolution Radiometer (AVHRR)*. Taylor & Francis, London.

De Beurs KM, Henebry GM (2004) Trend analysis of the Pathfinder AVHRR Land (PAL) NDVI data for the deserts of central Asia. *IEEE Geoscience and Remote Sensing Letters*, **1**, 282–286.

De Beurs KM, Henebry GM (2005) A statistical framework for the analysis of long image time series. *International Journal of Remote Sensing*, **26**, 1551–1573.

De Beurs KM, Wright CK, Henebry GM (2009) Dual scale trend analysis for evaluating climatic and anthropogenic effects on the vegetated land surface in Russia and Kazakhstan. *Environmental Research Letters*, **4**, 045012.

De Jong R, De Bruin S, De Wit A, Schaepman ME, Dent DL (2011a) Analysis of monotonic greening and browning trends from global NDVI time-series. *Remote Sensing of Environment*, **115**, 692–702.

De Jong R, Verbesselt J, Schaepman ME, De Bruin S (2011b) *Detection of Breakpoints in Global NDVI time series*. In: 34th International Symposium on Remote Sensing of Environment (ISRSE). 10–15 April 2011, Sydney, Australia.

Dendoncker N, Schmit C, Rounsevell M (2008) Exploring spatial data uncertainties in land-use change scenarios. *International Journal of Geographical Information Science*, **22**, 1013–1030.

Domenikiotis C, Loukas A, Dalezios NR (2003) The use of NOAA/AVHRR satellite data for monitoring and assessment of forest fires and floods. *Natural Hazards and Earth System Sciences*, **3**, 115–128.

Donohue RJ, Mcvicar TR, Roderick ML (2009) Climate-related trends in Australian vegetation cover as inferred from satellite observations, 1981-2006. *Global Change Biology*, **15**, 1025–1039.

Fensholt R, Rasmussen K (2011) Analysis of trends in the Sahelian 'rain-use efficiency' using GIMMS NDVI, RFE and GPCP rainfall data. *Remote Sensing of Environment*, **115**, 438–451.

Fensholt R, Rasmussen K, Nielsen TT, Mbow C (2009) Evaluation of earth observation based long term vegetation trends - Intercomparing NDVI time series trend analysis consistency of Sahel from AVHRR GIMMS, Terra MODIS and SPOT VGT data. *Remote Sensing of Environment*, **113**, 1242–1255.

Gobron N, Belward A, Pinty B, Knorr W (2010) Monitoring biosphere vegetation 1998-2009. *Geophysical Research Letters*, **37**, L15402.

Goetz SJ, Bunn AG, Fiske GJ, Houghton RA (2005) Satellite-observed photosynthetic trends across boreal North America associated with climate and fire disturbance. *Proceedings of the National Academy of Sciences of the United States of America*, **102**, 13521–13525.

Goetz SJ, Epstein HE, Bhatt US *et al.* (2011) Recent Changes in Arctic Vegetation: Satellite Observations and Simulation Model Predictions. In: *Eurasian Arctic Land Cover and Land Use in a Changing Climate* (eds Gutman G, Reissell A), pp. 9–36. Spring-Verlag, Amsterdam.

Hansen J, Ruedy R, Sato M, Lo K (2010) Global surface temperature change. *Reviews of Geophysics*, **48**, RG4004 4001–4029.

Haywood J, Randall J (2008) *Trending seasonal data with multiple structural breaks*. NZ visitor arrivals and the minimal effects of 9/11. In: Research report 08/10. University of Wellington, Victoria, New Zealand, 26 p.

Herrmann SM, Anyamba A, Tucker CJ (2005) Recent trends in vegetation dynamics in the African Sahel and their relationship to climate. *Global Environmental Change Part A*, **15**, 394–404.

Heumann BW, Seaquist JW, Eklundh L, Jönsson P (2007) AVHRR derived phenological change in the Sahel and Soudan, Africa, 1982–2005. *Remote Sensing of Environment*, **108**, 385–392.

Holben BN (1986) Characteristics of maximum-value composite images from temporal AVHRR data. *International Journal of Remote Sensing*, **7**, 1417–1434.

Huete AR, Huiqing L, Van Leeuwen WJD (1997) The use of vegetation indices in forested regions: issues of linearity and saturation. In: *Geoscience and Remote Sensing Symposium (IGARSS)*. 3–8 Aug. 1997, pp. 1966–1968. IEEE International, Singapore.

Jung M, Reichstein M, Ciais P *et al.* (2010) Recent decline in the global land evapotranspiration trend due to limited moisture supply. *Nature*, **467**, 951–954.

Kasischke ES, French NHF, Harrell P, Christensen NL Jr, Ustin SL, Barry D (1993) Monitoring of wildfires in Boreal Forests using large area AVHRR NDVI composite image data. *Remote Sensing of Environment*, **45**, 61–71.

Kaufmann RK, Zhou L, Knyazikhin Y, Shabanov V, Myneni RB, Tucker CJ (2000) Effect of orbital drift and sensor changes on the time series of AVHRR vegetation index data. *IEEE Transactions on Geoscience and Remote Sensing*, **38**, 2584–2597.

Lloyd AH, Bunn AG (2007) Responses of the circumpolar boreal forest to 20th century climate variability. *Environmental Research Letters*, **2**, 045013.

Loveland TR, Belward AS (1997) The International Geosphere Biosphere Programme Data and Information System global land cover data set (DISCover). *Acta Astronautica*, **41**, 681–689.

Loveland TR, Reed BC, Brown JF, Ohlen DO, Zhu Z, Yang L, Merchant JW (2000) Development of a global land cover characteristics database and IGBP DISCover from 1 km AVHRR data. *International Journal of Remote Sensing*, **21**, 1303–1330.

Lucht W, Prentice IC, Myneni RB *et al.* (2002) Climatic control of the high-latitude vegetation greening trend and Pinatubo effect. *Science*, **296**, 1687–1689.

Myneni RB, Hall FG, Sellers PJ, Marshak AL (1995) The interpretation of spectral vegetation indexes. *IEEE Transactions on Geoscience and Remote Sensing*, **33**, 481–486.

Myneni RB, Keeling CD, Tucker CJ, Asrar G, Nemani RR (1997) Increased plant growth in the northern high latitudes from 1981 to 1991. *Nature*, **386**, 698–702.

Nelson GC, Bennett E, Berhe AA *et al.* (2006) Anthropogenic drivers of ecosystem change: an overview. *Ecology & Society*, **11**, 29.

Nemani RR, Keeling CD, Hashimoto H *et al.* (2003) Climate-driven increases in global terrestrial net primary production from 1982 to 1999. *Science*, **300**, 1560–1563.

Nicholson S (2000) Land surface processes and Sahel climate. *Reviews of Geophysics*, **38**, 117–138.

Niemi GJ, Mcdonald ME (2004) Application of ecological indicators. *Annual Review of Ecology, Evolution and Systematics*, **35**, 89–111.

Olsson L, Eklundh L, Ardö J (2005) A recent greening of the Sahel – trends, patterns and potential causes. *Journal of Arid Environments*, **63**, 556–566.

Paruelo JM, Epstein HE, Lauenroth WK, Burke IC (1997) ANPP estimates from NDVI for the central grassland region of the United States. *Ecology*, **78**, 953–958.

Paruelo JM, Garbulsky MF, Guerschman JP, Jobbágy EG (2004) Two decades of Normalized Difference Vegetation Index changes in South America: identifying the imprint of global change. *International Journal of Remote Sensing*, **25**, 2793–2806.

Pettorelli N, Vik JO, Mysterud A, Gaillard J-M, Tucker CJ, Stenseth NC (2005) Using the satellite-derived NDVI to assess ecological responses to environmental change. *Trends in Ecology & Evolution*, **20**, 503–510.

Pilifosova O, Eserkepova I, Dolgih S (1997) Regional climate change scenarios under global warming in Kazakhstan. *Climatic Change*, **36**, 23–40.

Potter CS, Klooster S, Brooks V (1999) Interannual variability in terrestrial net primary production: exploration of trends and controls on regional to global scales. *Ecosystems*, **2**, 36–48.

Potter C, Tan P-N, Steinbach M, Klooster S, Kumar V, Myneni R, Genovese V (2003) Major disturbance events in terrestrial ecosystems detected using global satellite data sets. *Global Change Biology*, **9**, 1005–1021.

R Development Core Team (2011) *R: A Language and Environment for Statistical Computing*. R Foundation for Statistical Computing, Vienna, Austria. ISBN 3-900051-07-0. Available at: http://www.R-project.org/ (accessed 20 August 2011).

Running SW, Loveland TR, Pierce LL (1994) A vegetation classification logic based on remote sensing for use in global biogeochemical models. *Ambio*, **23**, 77–81.

Samanta A, Costa MH, Nunes EL, Vieira SA, Xu L, Myneni RB (2011) Comment on "Drought-induced reduction in global terrestrial net primary production from 2000 through 2009". *Science*, **333**, 1093.

Scheffer M, Carpenter S, Foley JA, Folke C, Walker B (2001) Catastrophic shifts in ecosystems. *Nature*, **413**, 591–596.

Schimel DS, House JI, Hibbard KA *et al.* (2001) Recent patterns and mechanisms of carbon exchange by terrestrial ecosystems. *Nature*, **414**, 169–172.

Schwarz G (1978) Estimating the Dimension of a Model. *The Annals of Statistics*, **6**, 461–464.

Sjöström M, Ardö J, Arneth A *et al.* (2011) Exploring the potential of MODIS EVI for modeling gross primary production across African ecosystems. *Remote Sensing of Environment*, **115**, 1081–1089.

Slayback DA, Pinzon JE, Los SO, Tucker CJ (2003) Northern hemisphere photosynthetic trends 1982–99. *Global Change Biology*, **9**, 1–15.

Sobrino JA, Raissouni N, Li Z-L (2001) A comparative study of land surface emissivity retrieval from NOAA data. *Remote Sensing of Environment*, **75**, 256–266.

Soden BJ, Wetherald RT, Stenchikov GL, Robock A (2002) Global cooling after the eruption of Mount Pinatubo: a test of climate feedback by water vapor. *Science*, **296**, 727–730.

Stenchikov GL, Kirchner I, Robock A *et al.* (1998) Radiative forcing from the 1991 Mount Pinatubo volcanic eruption. *Journal of Geophysical Research*, **103**, 13837–13857.

Tucker CJ (1979) Red and photographic infrared linear combinations for monitoring vegetation. *Remote Sensing of Environment*, **8**, 27–150.

Tucker CJ, Pinzon JE, Brown ME (2004) Global Inventory Modeling and Mapping Studies, NA94apr15b.n11-VIg, 2.0, *Global Land Cover Facility*, University of Maryland, College Park, Maryland.

Tucker C, Pinzon J, Brown M *et al.* (2005) An extended AVHRR 8km NDVI dataset compatible with MODIS and SPOT vegetation NDVI data. *International Journal of Remote Sensing*, **26**, 4485–4498.

Turner BL, Lambin EF, Reenberg A (2007) The emergence of land change science for global environmental change and sustainability. *Proceedings of the National Academy of Sciences*, **104**, 20666–20671.

Venables WN, Ripley BD (2002) *Modern Applied Statistics with S* (4th edn). Springer, New York, USA, 495 p.

Verbesselt J, Hyndman R, Newnham G, Culvenor D (2010a) Detecting trend and seasonal changes in satellite image time series. *Remote Sensing of Environment*, **114**, 106–115.

Verbesselt J, Hyndman R, Zeileis A, Culvenor D (2010b) Phenological change detection while accounting for abrupt and gradual trends in satellite image time series. *Remote Sensing of Environment*, **114**, 2970–2980.

Verburg PH, Neumann K, Nol L (2011) Challenges in using land use and land cover data for global change studies. *Global Change Biology*, **17**, 974–989.

Viglizzo EF, Frank FC, Carreno LV *et al.* (2011) Ecological and environmental footprint of 50 years of agricultural expansion in Argentina. *Global Change Biology*, **17**, 959–973.

Viles HA, Goudie AS (2003) Interannual, decadal and multidecadal scale climatic variability and geomorphology. *Earth-Science Reviews*, **61**, 105–131.

Wang X, Piao S, Ciais P, Li J, Friedlingstein P, Koven C, Chen A (2011) Spring temperature change and its implication in the change of vegetation growth in North America from 1982 to 2006. *Proceedings of the National Academy of Sciences*, **108**, 1240–1245.

Wessels KJ, Prince SD, Malherbe J, Small J, Frost PE, Vanzyl D (2007) Can human-induced land degradation be distinguished from the effects of rainfall variability? A case study in South Africa. *Journal of Arid Environments*, **68**, 271–297.

Wolter K, Timlin MS (1998) Measuring the strength of enso events: How does 1997/98 rank? *Weather*, **53**, 315–324.

Woodward FI, Lomas MR, Quaife T (2008) Global responses of terrestrial productivity to contemporary climatic oscillations. *Philosophical Transactions of the Royal Society B: Biological Sciences*, **363**, 2779–2785.

Zeileis A, Kleiber C (2005) Validating multiple structural change models-a case study. *Journal of Applied Econometrics*, **20**, 685–690.

Zeileis A, Leisch F, Hornik K, Kleiber C (2002) Strucchange: an R package for testing for structural change in linear regression models. *Journal of Statistical Software*, **7**, 1–38.

Zhang R, Delworth TL (2006) Impact of Atlantic multidecadal oscillations on India/Sahel rainfall and Atlantic hurricanes. *Geophysical Research Letters*, **33**, L17712.

Zhang K, Kimball JS, Mu Q, Jones LA, Goetz SJ, Running SW (2009) Satellite based analysis of northern ET trends and associated changes in the regional water balance from 1983 to 2005. *Journal of Hydrology*, **379**, 92–110.

Zhao M, Running SW (2010) Drought-induced reduction in global terrestrial net primary production from 2000 through 2009. *Science*, **329**, 940–943.

Zhou L, Tucker CJ, Kaufmann RK, Slayback DA, Shabanov NV, Myneni RB (2001) Variations in northern vegetation activity inferred from satellite data of vegetation index during 1981 to 1999. *Journal of Geophysical Research*, **106**, 20269–20283.